BBN to today abundances (wikipedia)

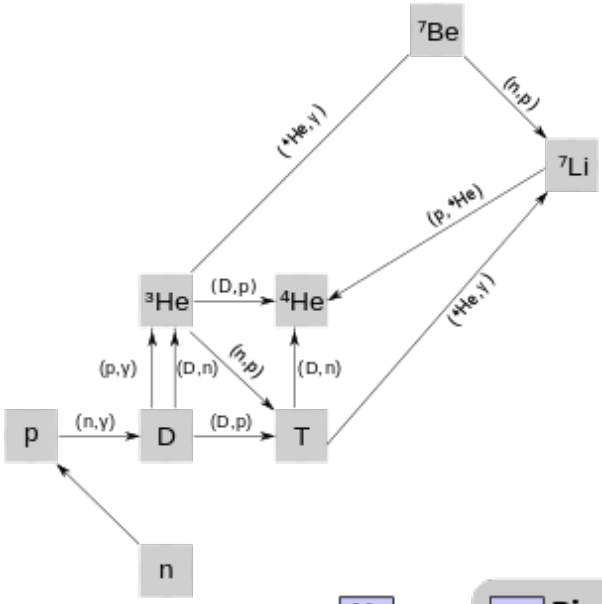

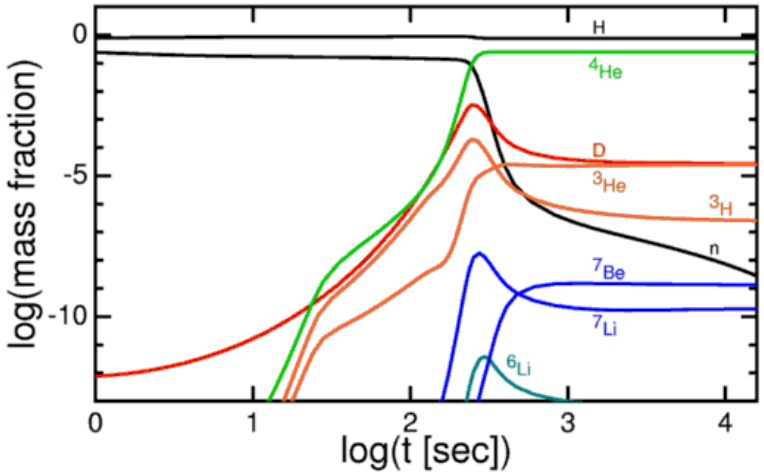

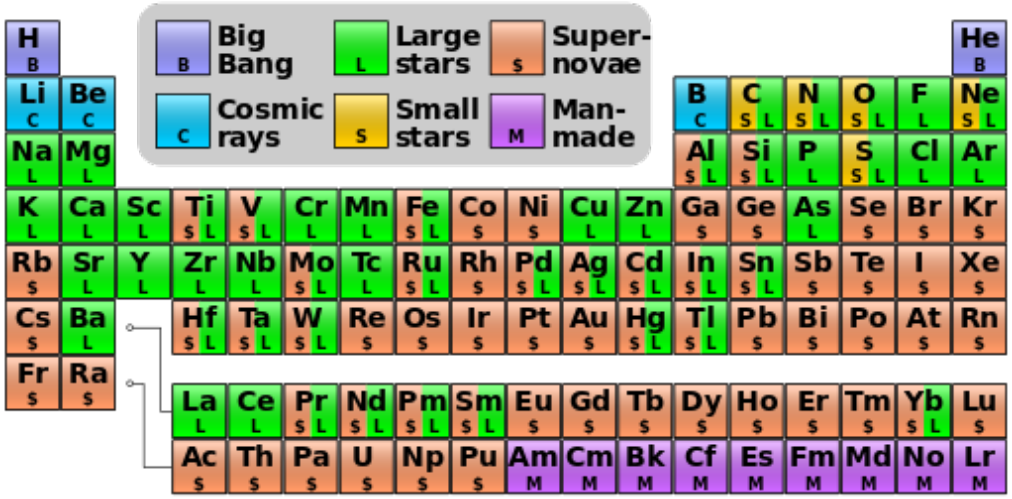

--> Stellar nucleosynthesis to create heavy elements (“metals”)

Metallicity vs redshift

http://adsabs.harvard.edu/abs/2014ARA%26A..52..415M

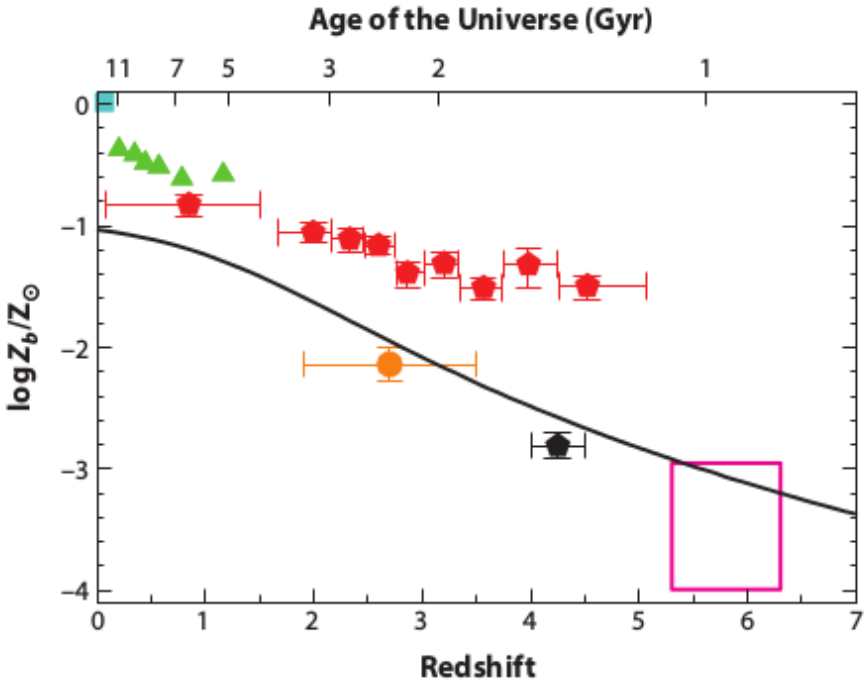

Mean metallicity of the Universe (in solar units): (solid curve) mass of heavy elements ever produced per cosmic baryon from our model SFH, for an assumed IMF-averaged yield of y = 0.02; (turquoise square) mass-weighted stellar metallicity in the nearby Universe from the SDSS (Gallazzi et al. 2008); (green triangles) mean iron abundances in the central regions of galaxy clusters (Balestra et al. 2007); (red pentagons) column density-weighted metallicities of the damped Lyα absorption systems (Rafelski et al. 2012); (orange dot) metallicity of the IGM as probed by O VI absorption in the Lyα forest (Aguirre et al. 2008); (black pentagon) metallicity of the IGM as probed by C IV absorption (Simcoe 2011); (magenta rectangle) metallicity of the IGM as probed by C IV and C II absorption (Ryan-Weber et al. 2009, Becker et al. 2011, Simcoe et al. 2011). Abbreviations: IGM, intergalactic medium; IMF, initial mass function; SDSS, Sloan Digital Sky Survey; SFH, star-formation history.

--> Metallicity related to star formation rate (SFR) and initial mass formation (IMF)

Star formation history (SFR)

http://adsabs.harvard.edu/abs/2014ARA%26A..52..415M

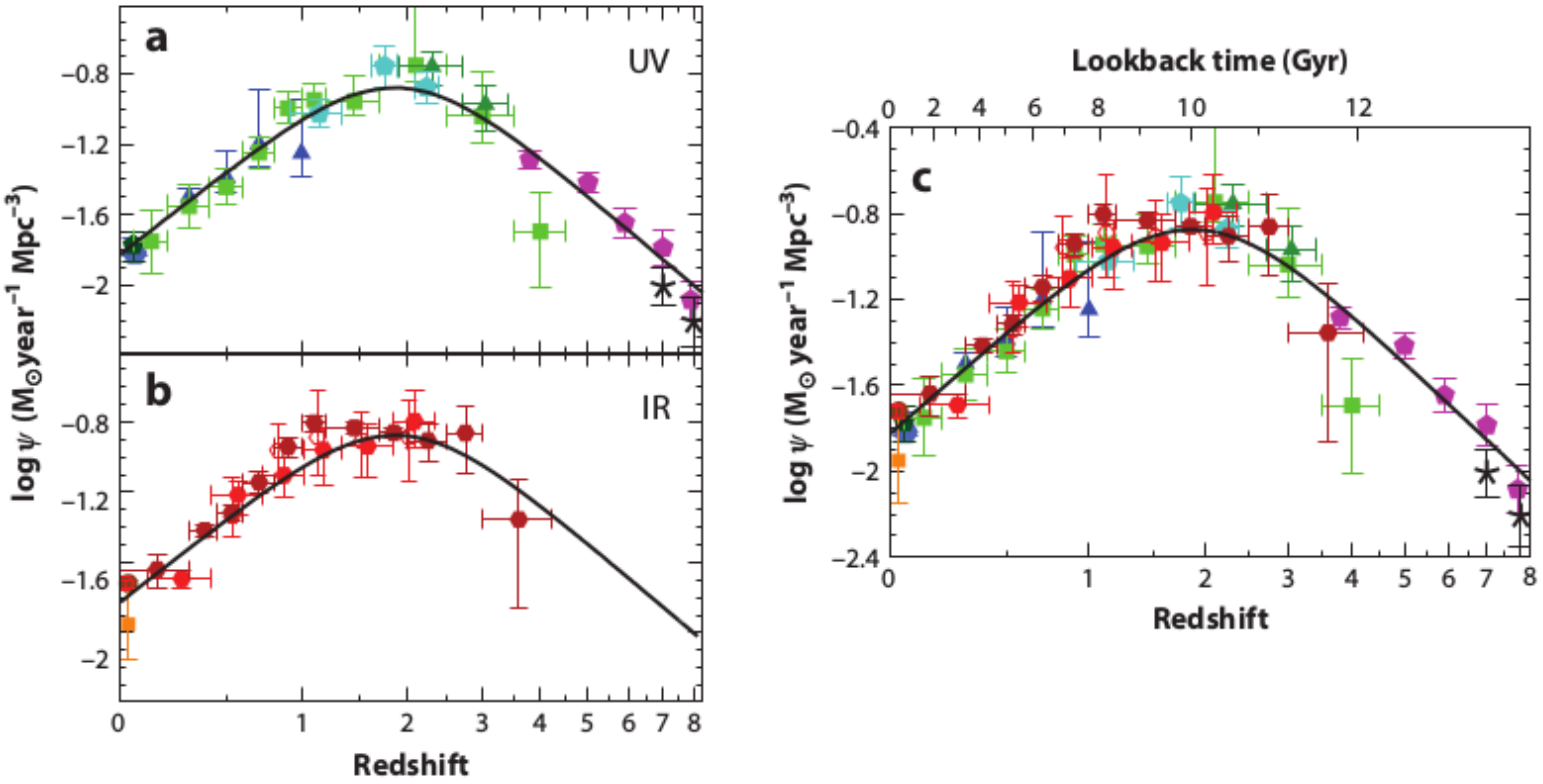

The history of cosmic star formation from (a) FUV, (b) IR, and (c) FUV+IR rest-frame measurements. The data points with symbols are given in Table 1. All UV luminosities have been converted to instantaneous SFR densities using the factor K FUV = 1.15×10^{-28} (see Equation 10), valid for a Salpeter IMF. FIR luminosities (8–1,000 μm) have been converted to instantaneous SFRs using the factor K IR = 4.5×10^{-44} (see Equation 11), also valid for a Salpeter IMF. The solid curve in the three panels plots the best-fit SFR density in Equation 15. Abbreviations: FIR, far-infrared; FUV, far-UV; IMF, initial mass function; IR, infrared; SFR, star-formation rate.

--> SFR peaks at z=2

Pop I, II, and III stars

http://adsabs.harvard.edu/abs/2014ARA%26A..52..415M

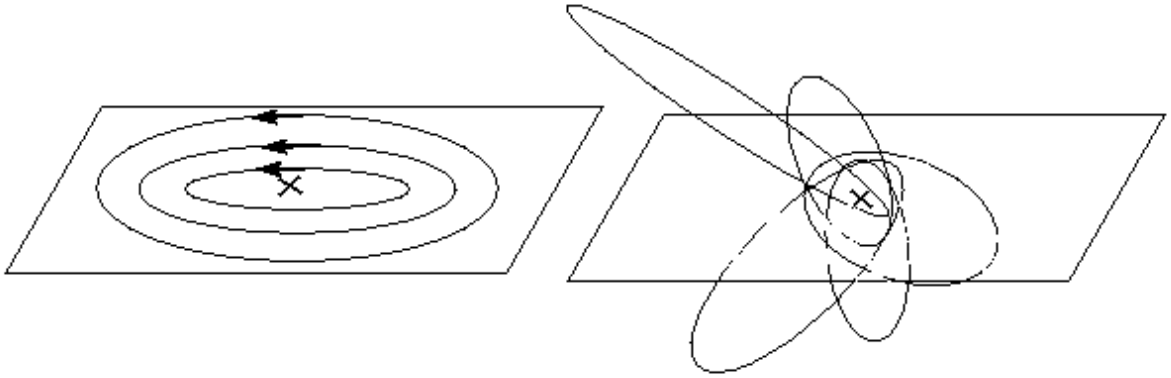

Population I stars: ordered motion. Circular orbits in the disk plane; younger, more metal-rich.

Population II stars: random motion. Eccentric orbits passing through disk plane; older, more metal-poor.

- Definition: Pop III = zero metallicity
  - IMF not observationally constrained at this time
  - We don't observe Pop III stars directly

- Interpretation of "fossil evidence" highly uncertain
  - Must rely on theory/simulations
  - Robust prediction: first stars were massive
    ... but not all Pop III stars may form this way

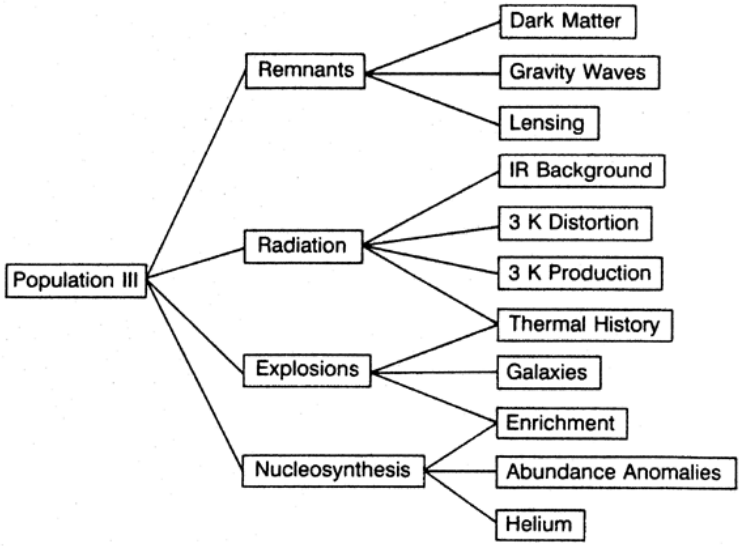

--> Pop III are a very peculiar population: they play an important role in cosmology

Search for Pop III stars

From Norman's talk

Disclaimer

- Notion of Pop III IMF is not well-defined
  - We don't observe Pop III stars
  - We believe Pop III stars formed in isolation in minihalos at high redshift……although some may be born binary stars
  - DM halos with enough mass to form a cluster of Pop III stars may be chemically enriched, and therefore form Pop II stars
- What is the sample we are averaging over?
  - Is there such a thing as a Pop III galaxy?
  - If not, we can define as a cosmic average <IMF(z)>
- Are we allowed to average over redshift too?
  - Duration of Pop III epoch is unknown
  - we can predict when it starts, but not when it ends

Search for Pop III stars

From Norman's talk

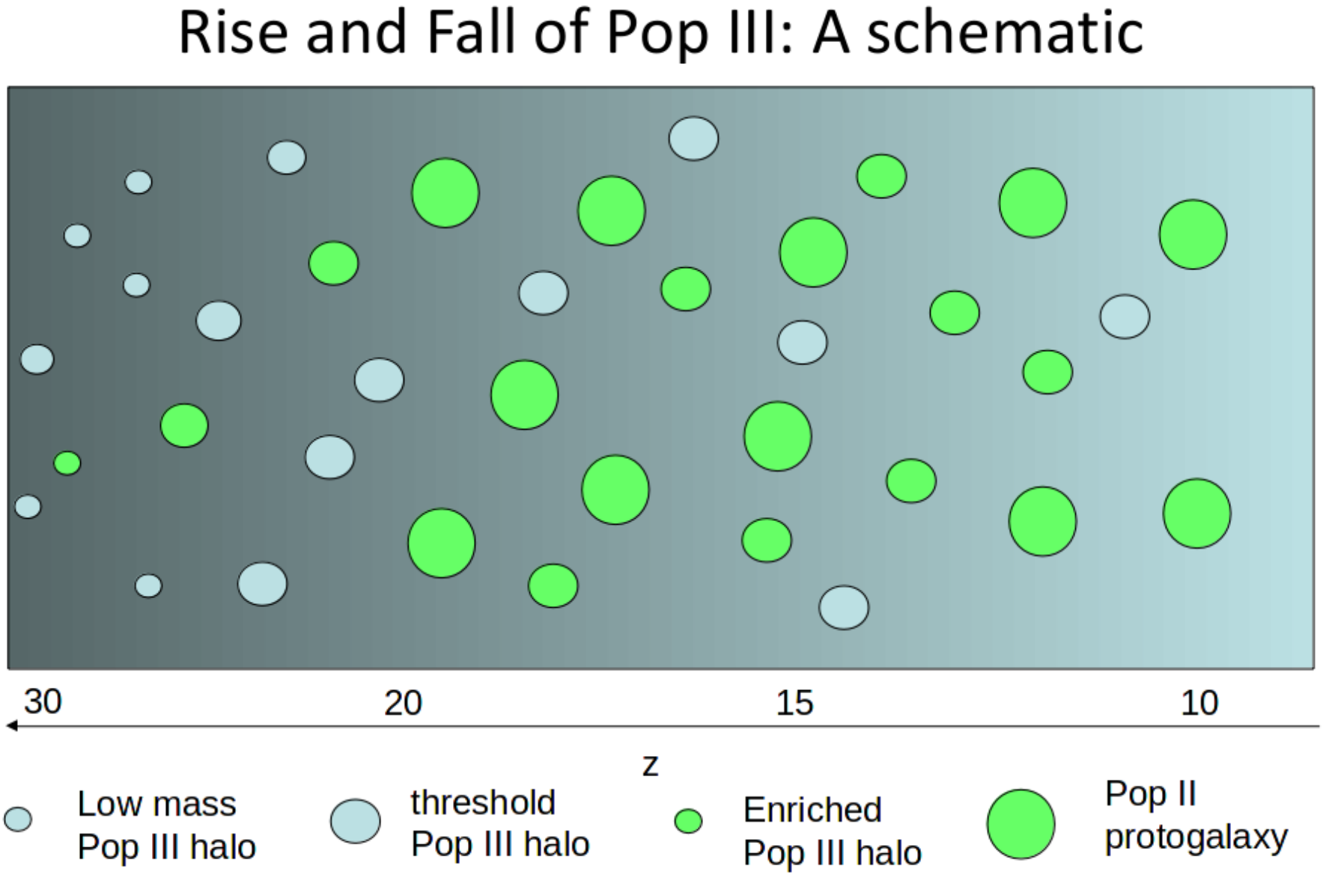

Ly alpha

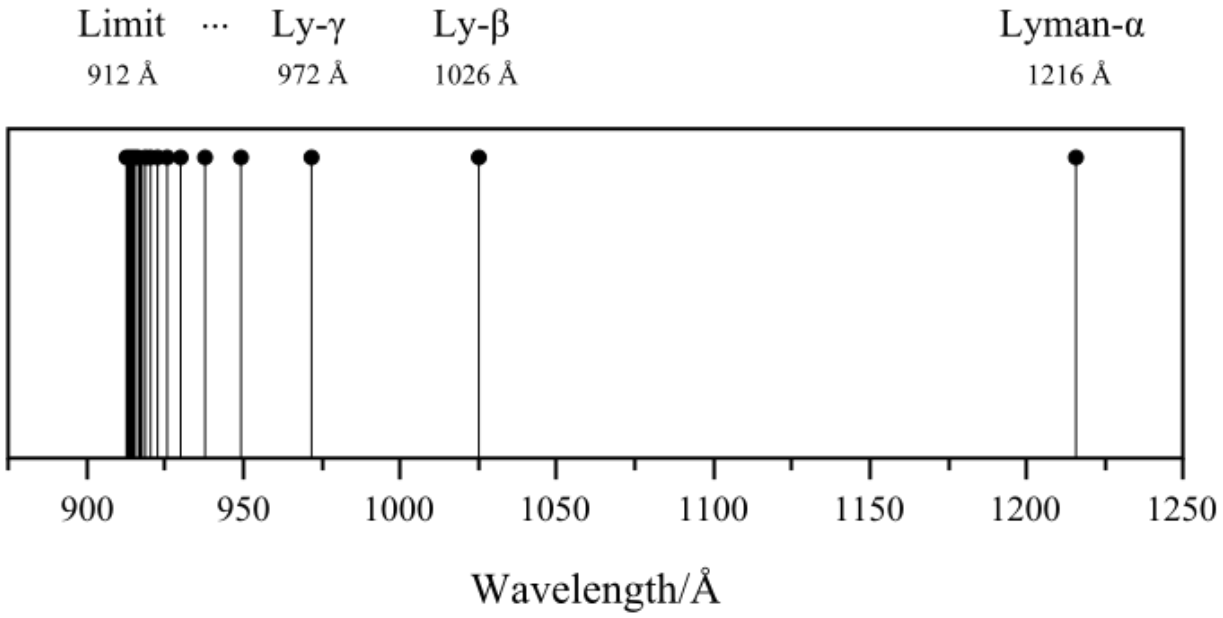

The Lyman series [edit]

The version of the Rydberg formula that generated the Lyman series was:[2]

$$\frac{1}{\lambda} = R_{\mathrm{H}}\left(1 - \frac{1}{n^2}\right) \qquad \left(R_{\mathrm{H}} \approx 1.0968{\times}10^{7}\,\mathrm{m}^{-1} \approx \frac{13.6\,\mathrm{eV}}{hc}\right)$$

Where n is a natural number greater than or equal to 2 (i.e., n = 2, 3, 4, ...).

Therefore, the lines seen in the image above are the wavelengths corresponding to n=2 on the right, to $n = \infty$ on the left (there are infinitely many spectral lines, but they become very dense as they approach to $n = \infty$ (Lyman limit), so only some of the first lines and the last one appear).

The wavelengths (nm) in the Lyman series are all ultraviolet:

n	2	3	4	5	6	7	8	9	10	11	∞, the Lyman limit
Wavelength (nm)	121.6	102.6	97.3	95.0	93.8	93.1	92.6	92.3	92.1	91.9	91.18

Ly alpha (LAE) emitters and absorbers

$$1 + z = \frac{\lambda}{1215.67\text{Å}}$$

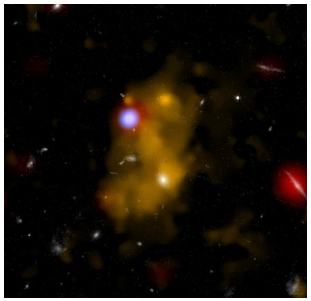

Lyα emitter (LAE)

- type of distant galaxy that emits Lyman-alpha radiation.
- thought to be the progenitors of most modern Milky Way type galaxies.
- found by an excess of their narrow-band flux at a wavelength interpreted as their z

Lyα forest (absorption) is a series of absorption lines (from neutral hydrogen) observed from distant galaxies and quasars.
Absorption systems with:

- N(HI)<$10^{17.2}$ cm^{-2}: Lyα forest lines
- $10^{17.2}$<N(HI) <$10^{20.3}$ cm^{-2}: Ly limit systems (LLS)
- N(HI)>$10^{20.3}$ cm^{-2}: damped Lyα systems (DLA)

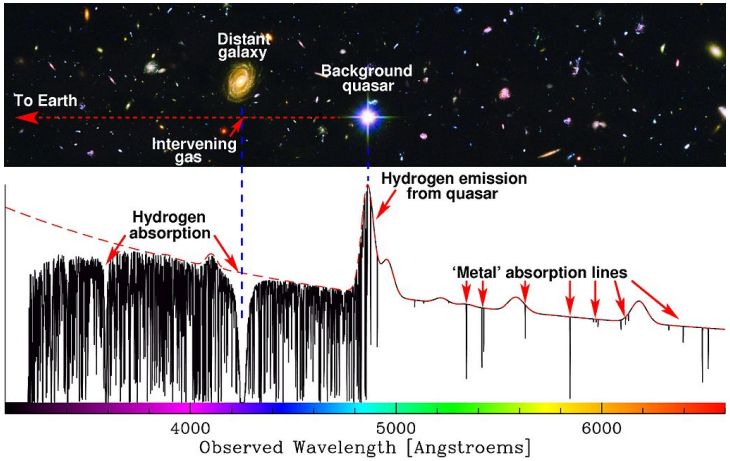

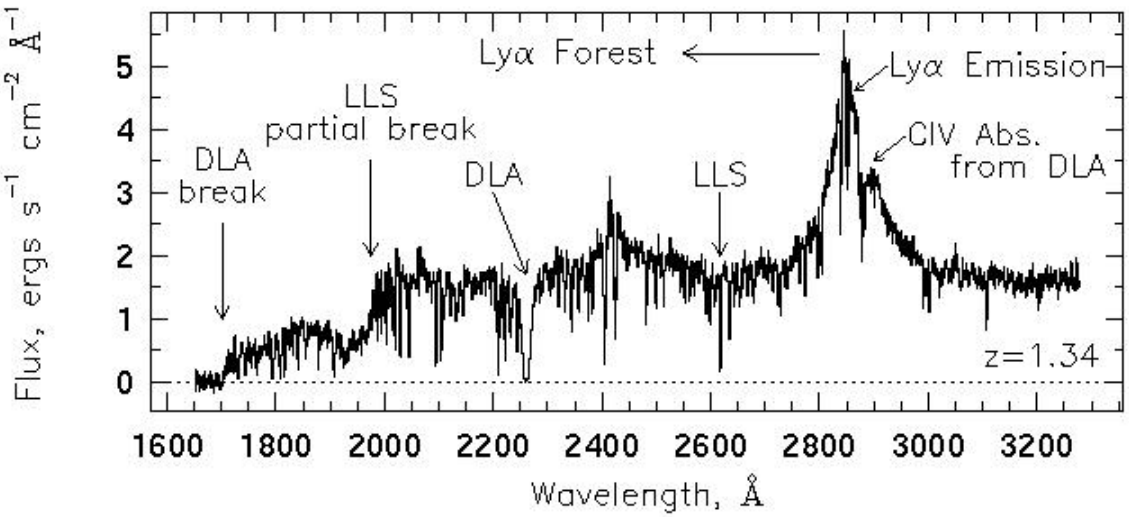

What is the Reionization Era?

A Schematic Outline of the Cosmic History

S.G. Djorgovski et al. & Digital Media Center, Caltech

Lyα and cosmology

http://adsabs.harvard.edu/abs/2014PASA...31...40D

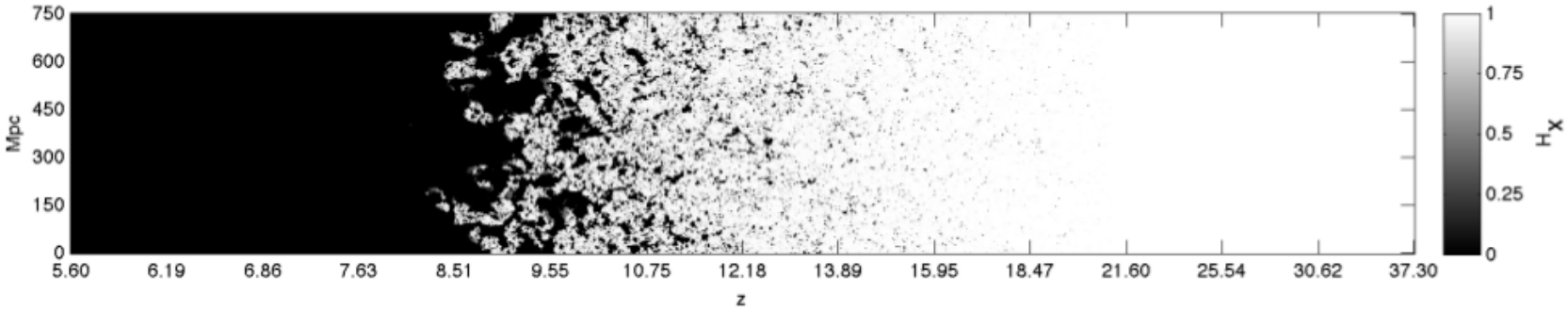

Figure 14: The predicted redshift evolution of the ionization state of the IGM in a realistic reionization model (*Credit: Figure kindly provided by Andrei Mesinger*). The white/black represents fully neutral/ionized intergalactic gas. This Figure demonstrates the inhomogeneous nature of the reionization process which took places over an extended range of redshifts: at $z > 16$ the first ionized regions formed around the most massive galaxies in the Universe (at that time). During the final stages of reionization - here at $z \sim 9$ the IGM contains ionized bubbles several tens of cMpc across.

• Lyα Forest grows denser and denser with redshift, until it leaves no flux behind and becomes a Gunn-Peterson Trough. This is the very end of reionization, because Lyα is very sensitive to even small amounts of residual HI.

• Lyα Forest can be used to trace the Dark Matter large scale structure of the Universe and its evolution.

• Damped Lyα Absorber systems can be used as a tracer of galaxy formation history complementary to observations in emission, because DLAs are selected by size rather than luminosity.

Star formation history (SFR)

http://adsabs.harvard.edu/abs/2014ARA%26A..52..415M

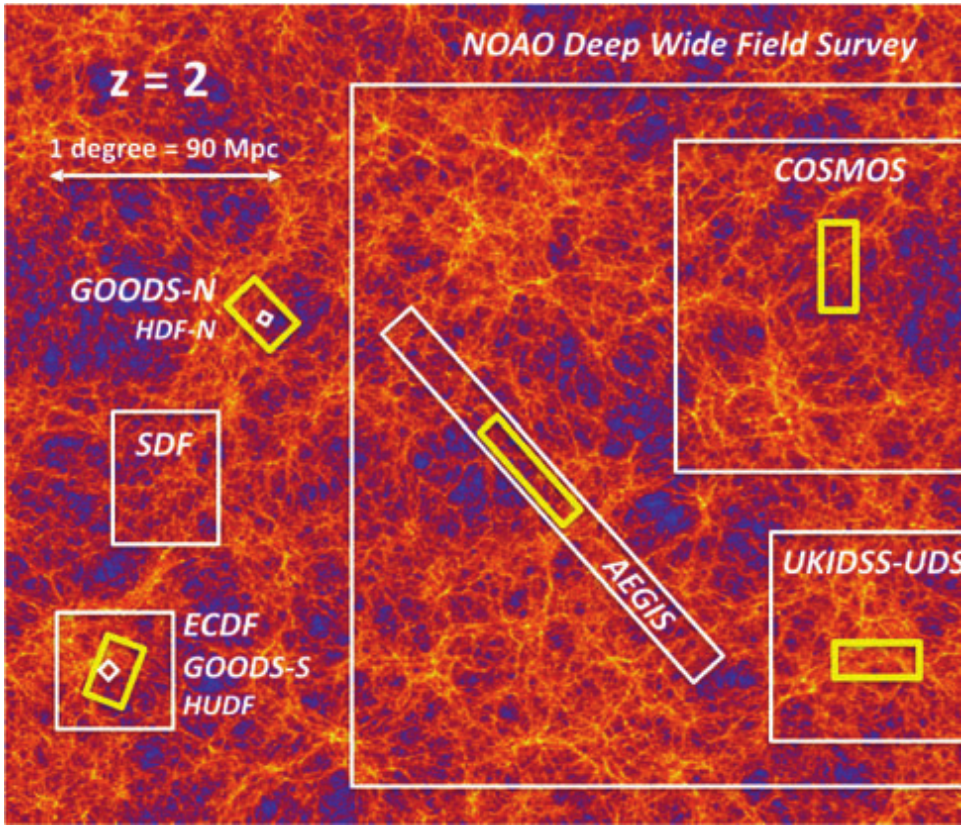

Relative sizes of the regions on the sky observed in several important surveys of the distant Universe. The two Great Observatories Origins Deep Survey (GOODS) fields, the Subaru Deep Field (SDF) and the Extended Chandra Deep Field South (ECDFS) are shown on the left. Very-deep surveys such as the Hubble Deep Field North (HDF-N) and the Hubble Ultradeep Field (HUDF) [Advanced Camera for Surveys (ACS) area shown], which are embedded within the GOODS fields, can detect fainter galaxies, but cover only very tiny regions on the sky. Other surveys such as the Cosmic Evolution Survey (COSMOS), the UK Infrared Deep Sky Survey (UKIDSS), the Ultradeep Survey (UDS), the All-Wavelength Extended Groth Strip International Survey (AEGIS), and the National Optical Astronomy Observatory (NOAO) Deep Wide Field Survey cover wider regions of the sky, usually to shallower depths, i.e., with less sensitivity to very faint galaxies. However, they encompass larger and perhaps more statistically representative volumes of the Universe. The yellow boxes indicate the five fields from the Cosmic Assembly Near-Infrared Deep Extragalactic Legacy Survey (CANDELS), each of which is embedded within another famous survey area.

Sobral et al. (2015)

Evidence for PIII-like stellar populations in the most luminous Lyα emitters at the epoch of reionization: spectroscopic confirmation [“Focus news” in Nature]

Methodology

– Multi-λ observations (COSMOS/Ultra VISTA field)

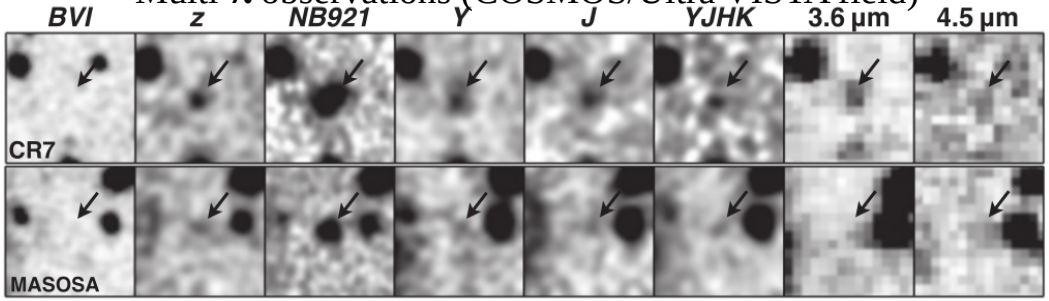

Figure 2. Thumbnails of both luminous Lyα emitters in the optical to MIR from left to right. Each thumbnail is 8 × 8″, corresponding to ∼44 × 44 kpc at $z \sim 6.6$. Not that while for MASOSA the Lyα emission line is detected by the NB921 filter at full transmission, for CR7 the Lyα is only detected at ∼50% transmission. Therefore the NB921 only captures ∼50% of the Lyα flux: the observed flux coming from the source is ∼2× larger.

– Flux comparison/ratio in various bands

Measurement[a]	CR7	MASOSA	Himiko
z_{spec} Lyα	$6.604^{+0.001}_{-0.003}$	6.541 ± 0.001	6.54
β UV slope	−2.3 ± 0.08	…	−2.0 ± 0.57
Lyα (FWHM, km s^{-1})	266 ± 15	386 ± 30	251 ± 21
Lyα ($EW_{0,obs,Y}$[b], Å)	211 ± 20	>206	78 ± 8
Lyα ($EW_{0,obs,spec}$, Å)	>230	>200	…
Lyα (Log_{10} L, erg s^{-1})	43.93 ± 0.05	43.38 ± 0.06	43.40 ± 0.07[c]
Lyα/N v	>70	…	…
He II/Lyα	0.23 ± 0.10	…	…
He II (EW_0, Å)	80 ± 20 (>20)	…	…
He II (FWHM, km s^{-1})	130 ± 30	…	…
He II/O III] 1663	>3	…	…
He II/C III] 1908	>2.5	…	…
z	25.35 ± 0.20	26.28 ± 0.37	25.86 ± 0.20[d]
NB921 2″ aperture	23.70 ± 0.04	23.84 ± 0.04	23.95 ± 0.02[e]
NB921 MAG-AUTO	23.24 ± 0.03	23.81 ± 0.03	23.55 ± 0.05[d]
Y	24.92 ± 0.13	>26.35	25.0 ± 0.35[f]
J	24.62 ± 0.10	>26.15	25.03 ± 0.25[d]
H	25.08 ± 0.14	>25.85	25.5 ± 0.35[f]
K	25.15 ± 0.15	>25.65	24.77 ± 0.29[d]
3.6 μm	23.86 ± 0.17	>25.6	23.69 ± 0.09[d]
4.5 μm	24.52 ± 0.61	>25.1	24.28 ± 0.19[d]

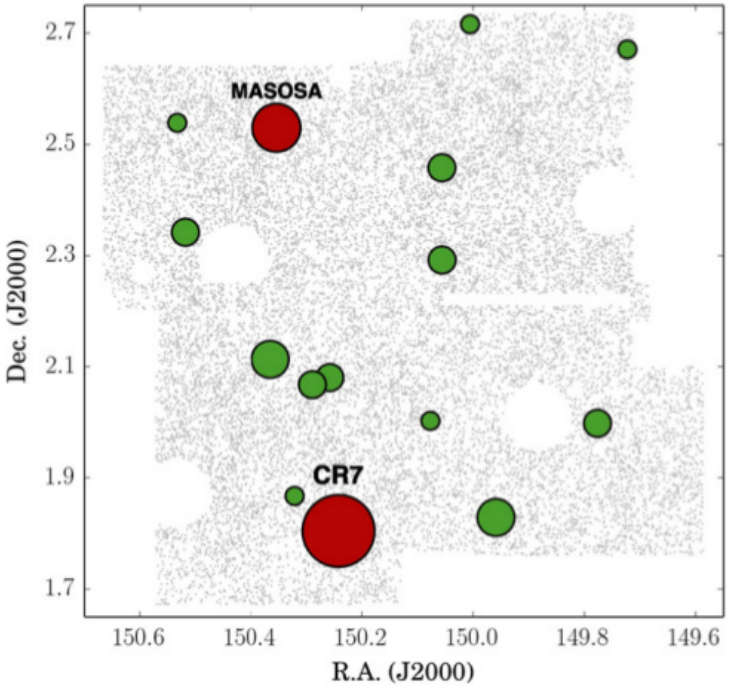

Figure 1. Projected positions on the sky of all Lyα candidates (green circles) found in the COSMOS/UltraVISTA field. The gray background points represent all detected sources with the NB921 filter, highlighting the masking applied (due to the presence of artifacts caused by bright stars and noisy regions, see Matthee et al. 2015). Lyα candidates are plotted with a symbol size proportional to their Lyα luminosity. CR7 and MASOSA are highlighted in red: these are the most luminous sources found in the field. Their coordinates

Sobral et al. (2015)

Evidence for PIII-like stellar populations in the most luminous Lyα emitters at the epoch of reionization: spectroscopic confirmation [“Focus news” in Nature]

Methodology

- Check if compatible with AGN, WR stars, etc. (it's not)
- Modelling of pristine and more evolved components

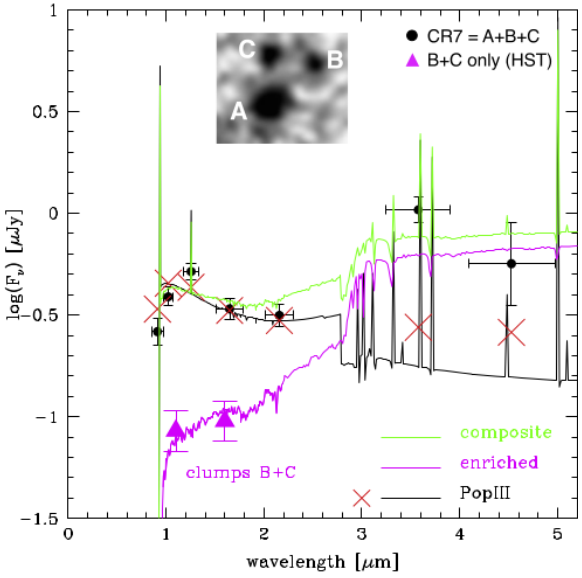

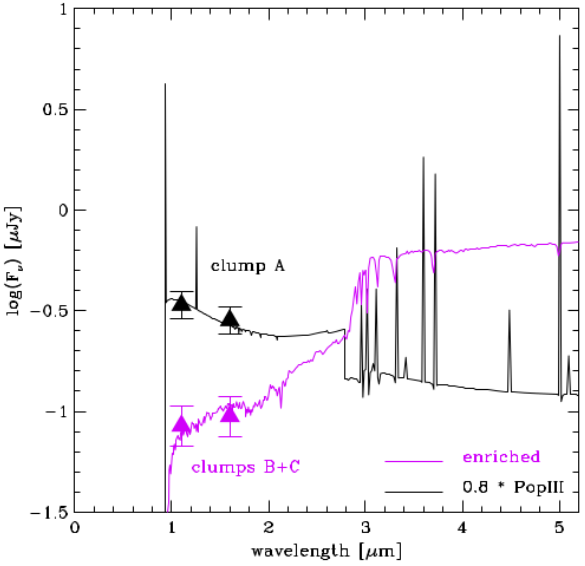

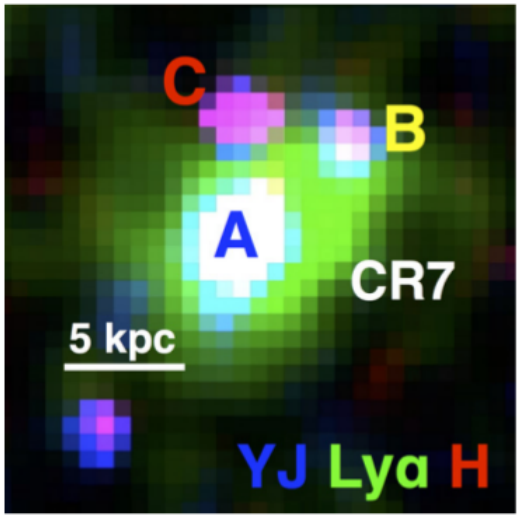

gure 7. False color composite of CR7 by using NB921/Suprime-cam imaging (Lyα) and two *HST*/WFC3 filters: F110W (*YJ*) and F160W (*H*). This

--> First “observation” of a Pop III population

--> before, expected to be visible only with James Webb telescope (launch 2018)

Crighton et al. (2016)

Possible Population III remnants at redshift 3.5

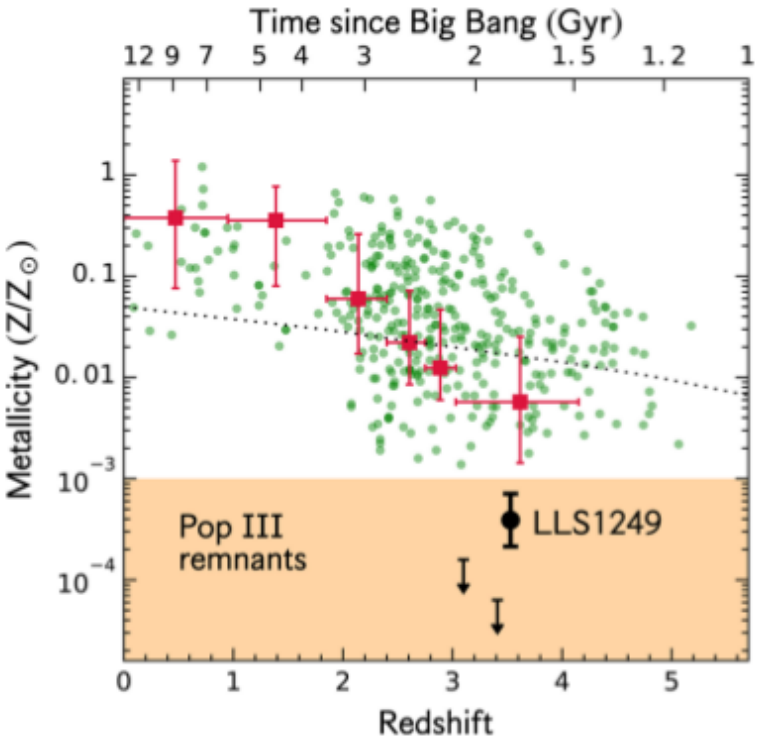

--> Lyα system with very low metallicity!

--> Suggests that LLS was enriched by a single PopIII event (near pristine abundances)